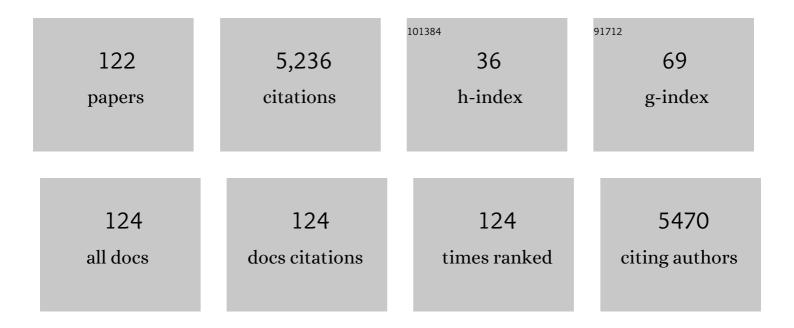
Yi-Xian Qin

List of Publications by Year in descending order

Source: https://exaly.com/author-pdf/116704/publications.pdf Version: 2024-02-01



ΥΙ-ΧΙΛΝ ΟΙΝ

#	Article	IF	CITATIONS
1	Longitudinal Intravital Imaging Through Clear Silicone Windows. Journal of Visualized Experiments, 2022, , .	0.2	5
2	Design and simulation of a 2-D array flexible ultrasound transducer system for tissue characterization – A pilot study. Medicine in Novel Technology and Devices, 2022, 13, 100106.	0.9	0
3	A universal post-treatment strategy for biomimetic composite hydrogel with anisotropic topological structure and wide range of adjustable mechanical properties. Materials Science and Engineering C, 2022, 133, 112654.	3.8	2
4	Biodegradable Zn–Sr alloys with enhanced mechanical and biocompatibility for biomedical applications. Smart Materials in Medicine, 2022, 3, 117-127.	3.7	12
5	Biomechanical Comparison of Krackow Repair and Percutaneous Achilles Repair System for Achilles Tendon Rupture Fixation: A Cadaveric and Finite Element Analysis Study. Foot & Ankle Orthopaedics, 2022, 7, 24730114221088502.	0.1	4
6	Thermal and NIR controlled flexible switching devices using a smart conductive composite hydrogel approach. Composites Science and Technology, 2022, 222, 109371.	3.8	15
7	Improved mechanical, degradation, and biological performances of Zn–Fe alloys as bioresorbable implants. Bioactive Materials, 2022, 17, 334-343.	8.6	7
8	High-strength and tough composite hydrogels reinforced by the synergistic effect of nano-doping and triple-network structures. European Polymer Journal, 2021, 142, 110122.	2.6	6
9	Calcium phosphate coatings enhance biocompatibility and degradation resistance of magnesium alloy: Correlating in vitro and in vivo studies. Bioactive Materials, 2021, 6, 1223-1229.	8.6	59
10	Evaluation of nucleus pulposus fluid velocity and pressure alteration induced by cartilage endplate sclerosis using a poro-elastic finite element analysis. Biomechanics and Modeling in Mechanobiology, 2021, 20, 281-291.	1.4	8
11	Piezo1 channel activation in response to mechanobiological acoustic radiation force in osteoblastic cells. Bone Research, 2021, 9, 16.	5.4	40
12	Fe3+, NIR light and thermal responsive triple network composite hydrogel with multi-shape memory effect. Composites Science and Technology, 2021, 206, 108653.	3.8	25
13	Longitudinal effects of low-intensity pulsed ultrasound on osteoporosis and osteoporotic bone defect in ovariectomized rats. Ultrasonics, 2021, 113, 106360.	2.1	14
14	Mechanobiological modulation of in situ and in vivo osteocyte calcium oscillation by acoustic radiation force. Annals of the New York Academy of Sciences, 2020, 1460, 68-76.	1.8	6
15	Therapeutic Effects of Low-Intensity Pulsed Ultrasound on Osteoporosis in Ovariectomized Rats: Intensity-Dependent Study. Ultrasound in Medicine and Biology, 2020, 46, 108-121.	0.7	19
16	InÂVivo Models of Muscle Stimulation and Mechanical Loading in Bone Mechanobiology. , 2020, , 117-136.		1
17	Evolution of metallic cardiovascular stent materials: A comparative study among stainless steel, magnesium and zinc. Biomaterials, 2020, 230, 119641.	5.7	113
18	Osteoclastic activity was associated with the development of steroid-induced osteonecrosis of femoral head. Artificial Cells, Nanomedicine and Biotechnology, 2020, 48, 1036-1046.	1.9	11

#	Article	IF	CITATIONS
19	Porous tantalum rod implantation is associated with low survival rates in patients with type C2 osteonecrosis of the femoral head but has no effect on the clinical outcome of conversion total hip arthroplasty: a retrospective study with an average 8-year follow-up. BMC Musculoskeletal Disorders, 2020, 21, 841.	0.8	6
20	Lowâ€intensity pulsed ultrasound protects subchondral bone in rabbit temporomandibular joint osteoarthritis by suppressing TGFâ€î21/Smad3 pathway. Journal of Orthopaedic Research, 2020, 38, 2505-2512.	1.2	11
21	Porous zinc scaffolds for bone tissue engineering applications: A novel additive manufacturing and casting approach. Materials Science and Engineering C, 2020, 110, 110738.	3.8	75
22	Quantitative ultrasound imaging monitoring progressive disuse osteopenia and mechanical stimulation mitigation in calcaneus region through a 90-day bed rest human study. Journal of Orthopaedic Translation, 2019, 18, 48-58.	1.9	13
23	Functional disuse initiates medullary endosteal micro-architectural impairment in cortical bone characterized by nanoindentation. Journal of Bone and Mineral Metabolism, 2019, 37, 1048-1057.	1.3	4
24	A Composite Hydrogel with High Mechanical Strength, Fluorescence, and Degradable Behavior for Bone Tissue Engineering. Polymers, 2019, 11, 1112.	2.0	47
25	Utilization of Finite Element Analysis for Articular Cartilage Tissue Engineering. Materials, 2019, 12, 3331.	1.3	14
26	Engineered nanomedicine for neuroregeneration: light emitting diode-mediated superparamagnetic iron oxide-gold core-shell nanoparticles functionalized by nerve growth factor. Nanomedicine: Nanotechnology, Biology, and Medicine, 2019, 21, 102052.	1.7	22
27	Mechanical Strength, Biodegradation, and in Vitro and in Vivo Biocompatibility of Zn Biomaterials. ACS Applied Materials & Interfaces, 2019, 11, 6809-6819.	4.0	111
28	Plasma C-terminal cross-linking telopeptide of type II collagen as a biomarker in advanced stages of femoral head osteonecrosis. Biomedicine and Pharmacotherapy, 2019, 111, 1213-1220.	2.5	5
29	Biofunctionalization of metallic implants by calcium phosphate coatings. Bioactive Materials, 2019, 4, 196-206.	8.6	173
30	Interfacial Zinc Phosphate is the Key to Controlling Biocompatibility of Metallic Zinc Implants. Advanced Science, 2019, 6, 1900112.	5.6	95
31	A Biomechanical Comparison of Alternative Graft Preparations for All-Inside Anterior Cruciate Ligament Reconstruction. Arthroscopy - Journal of Arthroscopic and Related Surgery, 2019, 35, 1547-1554.	1.3	9
32	Enhanced cytocompatibility and antibacterial property of zinc phosphate coating on biodegradable zinc materials. Acta Biomaterialia, 2019, 98, 174-185.	4.1	148
33	Elevated plasma cartilage oligomeric matrix protein (COMP) level are associated with the progression of non-traumatic osteonecrosis of femoral head. Clinica Chimica Acta, 2019, 490, 214-221.	0.5	7
34	Zinc-Based Biomaterials for Regeneration and Therapy. Trends in Biotechnology, 2019, 37, 428-441.	4.9	243
35	Retention of osteocytic micromorphology by sclerostin antibody in a concurrent ovariectomy and functional disuse model. Annals of the New York Academy of Sciences, 2019, 1442, 91-103.	1.8	9
36	Mitigation of Articular Cartilage Degeneration and Subchondral Bone Sclerosis in Osteoarthritis Progression Using Low-Intensity Ultrasound Stimulation. Ultrasound in Medicine and Biology, 2019, 45, 148-159.	0.7	8

#	Article	IF	CITATIONS
37	Effects of facet joint degeneration on stress alterations in cervical spine C5–C6: A finite element analysis. Mathematical Biosciences and Engineering, 2019, 16, 7447-7457.	1.0	9
38	An investigation of shock wave therapy and lowâ€intensity pulsed ultrasound on fracture healing under reduced loading conditions in an ovine model. Journal of Orthopaedic Research, 2018, 36, 921-929.	1.2	8
39	Promoting neuroregeneration by applying dynamic magnetic fields to a novel nanomedicine: Superparamagnetic iron oxide (SPIO)-gold nanoparticles bounded with nerve growth factor (NGF). Nanomedicine: Nanotechnology, Biology, and Medicine, 2018, 14, 1337-1347.	1.7	61
40	Acceleration of Bone Defect Healing and Regeneration by Low-Intensity Ultrasound Radiation Force in a Rat Tibial Model. Ultrasound in Medicine and Biology, 2018, 44, 2646-2654.	0.7	15
41	Association of reduced sclerostin expression with collapse process in patients with osteonecrosis of the femoral head. International Orthopaedics, 2018, 42, 1675-1682.	0.9	13
42	MC3T3 infiltration and proliferation in bovine trabecular scaffold regulated by dynamic flow bioreactor and augmented by low-intensity pulsed ultrasound. Journal of Orthopaedic Translation, 2018, 14, 16-22.	1.9	6
43	Zinc regulates vascular endothelial cell activity through zinc-sensing receptor ZnR/GPR39. American Journal of Physiology - Cell Physiology, 2018, 314, C404-C414.	2.1	64
44	Non-Enzymatic Glycation Crosslinking Affects Human Keratoconus Fibroblasts Behavior In Vitro. Journal of Biomaterials and Tissue Engineering, 2018, 8, 1334-1341.	0.0	1
45	Layer-by-layer, ultrasonic spray assembled 2D and 3D chemically crosslinked carbon nanotubes and graphene. Journal of Materials Research, 2017, 32, 370-382.	1.2	6
46	Novel Spiked-Washer Repair Is Biomechanically Superior to Suture and Bone Tunnels for Arcuate Fracture Repair. Journal of Orthopaedic Trauma, 2017, 31, e81-e85.	0.7	8
47	Effect of capsaicin-sensitive sensory neurons on bone architecture and mechanical properties in the rat hindlimb suspension model. Journal of Orthopaedic Translation, 2017, 10, 12-17.	1.9	7
48	<i>In situ</i> examination of osteoblast biomineralization on sulfonated polystyrene-modified substrates using Fourier transform infrared microspectroscopy. Biointerphases, 2017, 12, 031001.	0.6	1
49	SPIOâ€Au core–shell nanoparticles for promoting osteogenic differentiation of MC3T3â€E1 cells: Concentrationâ€dependence study. Journal of Biomedical Materials Research - Part A, 2017, 105, 3350-3359.	2.1	24
50	Spatial distribution and remodeling of elastic modulus of bone in micro-regime as prediction of early stage osteoporosis. Journal of Biomechanics, 2016, 49, 161-166.	0.9	6
51	Sclerostin antibody prevented progressive bone loss in combined ovariectomized and concurrent functional disuse. Bone, 2016, 87, 161-168.	1.4	36
52	Porous three-dimensional carbon nanotube scaffolds for tissue engineering. Journal of Biomedical Materials Research - Part A, 2015, 103, 3212-3225.	2.1	61
53	Dynamic acoustic radiation force retains bone structural and mechanical integrity in a functional disuse osteopenia model. Bone, 2015, 75, 8-17.	1.4	23
54	SHP2 regulates osteoclastogenesis by promoting preosteoclast fusion. FASEB Journal, 2015, 29, 1635-1645.	0.2	27

#	Article	IF	CITATIONS
55	Observation of sGAG content of human hip joint cartilage in different old age groups based on EPIC micro-CT. Connective Tissue Research, 2015, 56, 99-105.	1.1	11
56	Dynamic fluid flow induced mechanobiological modulation of in situ osteocyte calcium oscillations. Archives of Biochemistry and Biophysics, 2015, 579, 55-61.	1.4	31
57	Enhanced correlation between quantitative ultrasound and structural and mechanical properties of bone using combined transmission-reflection measurement. Journal of the Acoustical Society of America, 2015, 137, 1144-1152.	0.5	8
58	Fabrication and Cytocompatibility of In Situ Crosslinked Carbon Nanomaterial Films. Scientific Reports, 2015, 5, 10261.	1.6	18
59	Enhancement of Cell Ingrowth, Proliferation, and Early Differentiation in a Three-Dimensional Silicon Carbide Scaffold Using Low-Intensity Pulsed Ultrasound. Tissue Engineering - Part A, 2015, 21, 53-61.	1.6	31
60	Bone Tissue Engineering: Cell Motility, Vascularization, Micro-Nano Scaffolding, and Remodeling. BioMed Research International, 2014, 2014, 1-2.	0.9	4
61	Mechanotransduction in Musculoskeletal Tissue Regeneration: Effects of Fluid Flow, Loading, and Cellular-Molecular Pathways. BioMed Research International, 2014, 2014, 1-12.	0.9	47
62	Preliminary evidence of early bone resorption in a sheep model of acute burn injury: an observational study. Journal of Bone and Mineral Metabolism, 2014, 32, 136-141.	1.3	32
63	Principal trabecular structural orientation predicted by quantitative ultrasound is strongly correlated with \$\$upmu \$\$ μ FEA determined anisotropic apparent stiffness. Biomechanics and Modeling in Mechanobiology, 2014, 13, 961-971.	1.4	4
64	Effect of low-intensity pulsed ultrasound on biocompatibility and cellular uptake of chitosan-tripolyphosphate nanoparticles. Biointerphases, 2014, 9, 031016.	0.6	8
65	Interrelation between external oscillatory muscle coupling amplitude and in vivo intramedullary pressure related bone adaptation. Bone, 2014, 66, 178-181.	1.4	15
66	Dynamic fluid flow stimulation on cortical bone and alterations of the gene expressions of osteogenic growth factors and transcription factors in a rat functional disuse model. Archives of Biochemistry and Biophysics, 2014, 545, 154-161.	1.4	13
67	Axial Transmission Method for Long Bone Fracture Evaluation by Ultrasonic Guided Waves: Simulation, Phantom and inÂVitro Experiments. Ultrasound in Medicine and Biology, 2014, 40, 817-827.	0.7	18
68	Reversal of the Detrimental Effects of Simulated MicrogravityÂon Human Osteoblasts by Modified Low IntensityÂPulsed Ultrasound. Ultrasound in Medicine and Biology, 2013, 39, 804-812.	0.7	15
69	Tungsten disulfide nanotubes reinforced biodegradable polymers for bone tissue engineering. Acta Biomaterialia, 2013, 9, 8365-8373.	4.1	143
70	Dynamic hydraulic fluid stimulation regulated intramedullary pressure. Bone, 2013, 57, 137-141.	1.4	18
71	Prediction of trabecular bone qualitative properties using scanning quantitative ultrasound. Acta Astronautica, 2013, 92, 79-88.	1.7	22
72	Two-Dimensional Nanostructure-Reinforced Biodegradable Polymeric Nanocomposites for Bone Tissue Engineering. Biomacromolecules, 2013, 14, 900-909.	2.6	262

#	Article	IF	CITATIONS
73	The mechanical consequences of load bearing in the equine third metacarpal across speed and gait: the nonuniform distributions of normal strain, shear strain, and strain energy density. FASEB Journal, 2013, 27, 1887-1894.	0.2	21
74	Dynamic Fluid Flow Mechanical Stimulation Modulates Bone Marrow Mesenchymal Stem Cells. Bone Research, 2013, 1, 98-104.	5.4	15
75	Enhancement of Osteogenic Differentiation and Proliferation in Human Mesenchymal Stem Cells by a Modified Low Intensity Ultrasound Stimulation under Simulated Microgravity. PLoS ONE, 2013, 8, e73914.	1.1	82
76	Frequency Specific Ultrasound Attenuation is Sensitive to Trabecular Bone Structure. Ultrasound in Medicine and Biology, 2012, 38, 2198-2207.	0.7	7
77	Prediction of trabecular bone principal structural orientation using quantitative ultrasound scanning. Journal of Biomechanics, 2012, 45, 1790-1795.	0.9	14
78	Dynamic hydraulic flow stimulation on mitigation of trabecular bone loss in a rat functional disuse model. Bone, 2012, 51, 819-825.	1.4	36
79	Mechanobiological Modulation of Cytoskeleton and Calcium Influx in Osteoblastic Cells by Short-Term Focused Acoustic Radiation Force. PLoS ONE, 2012, 7, e38343.	1.1	53
80	Evaluation of a pulsed phase-locked loop system for noninvasive tracking of bone deformation under loading with finite element and strain analysis. Physiological Measurement, 2011, 32, 1301-1313.	1.2	4
81	Postural instability caused by extended bed rest is alleviated by brief daily exposure to low magnitude mechanical signals. Gait and Posture, 2011, 33, 429-435.	0.6	49
82	Alteration of contraction-to-rest ratio to optimize trabecular bone adaptation induced by dynamic muscle stimulation. Bone, 2011, 48, 399-405.	1.4	17
83	Mitigation of bone loss with ultrasound induced dynamic mechanical signals in an OVX induced rat model of osteopenia. Bone, 2011, 48, 1095-1102.	1.4	28
84	Effects of Phase Cancellation and Receiver Aperture Size on Broadband Ultrasonic Attenuation for Trabecular Bone InÂVitro. Ultrasound in Medicine and Biology, 2011, 37, 2116-2125.	0.7	17
85	A new algorithm for spatial impulse response of rectangular planar transducers. Ultrasonics, 2011, 51, 229-237.	2.1	6
86	Low-Intensity Amplitude Modulated Ultrasound Increases Osteoblastic Mineralization. Cellular and Molecular Bioengineering, 2011, 4, 81-90.	1.0	15
87	Extension of the distributed point source method for ultrasonic field modeling. Ultrasonics, 2011, 51, 571-580.	2.1	14
88	Quantitative ultrasound noninvasive investigation of trabecular organization and orientation. , 2011, , .		0
89	Phase cancellation and aperture size on broadband ultrasonic attenuation for trabecular bone assessment using a 2-D confocal synthetic array. , 2011, , .		0
90	Mechanobiologic acoustics on bone cellular and in vivo adaptation. , 2011, , .		0

#	Article	IF	CITATIONS
91	Skeletal nutrient vascular adaptation induced by external oscillatory intramedullary fluid pressure intervention. Journal of Orthopaedic Surgery and Research, 2010, 5, 18.	0.9	9
92	Mechanical signals as anabolic agents in bone. Nature Reviews Rheumatology, 2010, 6, 50-59.	3.5	368
93	Characterization of the trabecular bone structure using frequency modulated ultrasound pulse. Journal of the Acoustical Society of America, 2009, 125, 4071-4077.	0.5	16
94	Biomineralization of a Self-Assembled Extracellular Matrix for Bone Tissue Engineering. Tissue Engineering - Part A, 2009, 15, 355-366.	1.6	23
95	BMPâ€2 modulates βâ€catenin signaling through stimulation of <i>Lrp5</i> expression and inhibition of βâ€TrCP expression in osteoblasts. Journal of Cellular Biochemistry, 2009, 108, 896-905.	1.2	75
96	Intramedullary pressure and matrix strain induced by oscillatory skeletal muscle stimulation and its potential in adaptation. Journal of Biomechanics, 2009, 42, 140-145.	0.9	51
97	Evaluation of trabecular mechanical and microstructural properties in human calcaneal bone of advanced age using mechanical testing, μCT, and DXA. Journal of Biomechanics, 2008, 41, 368-375.	0.9	52
98	The effects of frequency-dependent dynamic muscle stimulation on inhibition of trabecular bone loss in a disuse model. Bone, 2008, 43, 1093-1100.	1.4	88
99	Stem Cells and Their Role in Bone Formation and Regeneration. , 2008, , 63-74.		0
100	Positron Emission Tomography of Bone in Small Animals. , 2008, , 331-346.		0
101	Functional Disuse Model for Musculoskeletal Adaptation. , 2008, , 457-475.		0
102	The Characterization of Cortical Bone Water Distribution and Structure Changes on Age, Microdamage, and Disuse by Nuclear Magnetic Resonance. , 2008, , 691-727.		0
103	Nanoindentation: Techniques and Technical Considerations for Musculoskeletal Research. , 2008, , 789-811.		0
104	Assessment of simulated and functional disuse on cortical bone by nuclear magnetic resonance. Advances in Space Research, 2007, 40, 1703-1710.	1.2	4
105	Determination of Ultrasound Phase Velocity in Trabecular Bone Using Time Dependent Phase Tracking Technique. Journal of Biomechanical Engineering, 2006, 128, 24-29.	0.6	6
106	Low-level mechanical signals and their potential as a non-pharmacological intervention for osteoporosis. Age and Ageing, 2006, 35, ii32-ii36.	0.7	91
107	Interrelationship of trabecular mechanical and microstructural properties in sheep trabecular bone. Journal of Biomechanics, 2005, 38, 1229-1237.	0.9	158
108	The influence of cortical end-plate on broadband ultrasound attenuation measurements at the human calcaneus using scanning confocal ultrasound. Journal of the Acoustical Society of America, 2005, 118, 1801-1807.	0.5	33

#	Article	IF	CITATIONS
109	Combining high-resolution micro-computed tomography with material composition to define the quality of bone tissue. Current Osteoporosis Reports, 2003, 1, 11-19.	1.5	76
110	Fluid pressure gradients, arising from oscillations in intramedullary pressure, is correlated with the formation of bone and inhibition of intracortical porosity. Journal of Biomechanics, 2003, 36, 1427-1437.	0.9	191
111	Adaptations of Trabecular Bone to Low Magnitude Vibrations Result in More Uniform Stress and Strain Under Load. Annals of Biomedical Engineering, 2003, 31, 12-20.	1.3	84
112	Quantity and Quality of Trabecular Bone in the Femur Are Enhanced by a Strongly Anabolic, Noninvasive Mechanical Intervention. Journal of Bone and Mineral Research, 2002, 17, 349-357.	3.1	266
113	The Pathway of Bone Fluid Flow as Defined by In Vivo Intramedullary Pressure and Streaming Potential Measurements. Annals of Biomedical Engineering, 2002, 30, 693-702.	1.3	89
114	Patterns of strain in the macaque tibia during functional activity. American Journal of Physical Anthropology, 2001, 116, 257-265.	2.1	135
115	Ultrasonic Wave Propagation in Trabecular Bone Predicted by the Stratified Model. Annals of Biomedical Engineering, 2001, 29, 781-790.	1.3	30
116	Inhibition of osteopenia by low magnitude, high-frequency mechanical stimuli. Drug Discovery Today, 2001, 6, 848-858.	3.2	129
117	Encoding of Location and Intensity of Noxious Indentation Into Rat Skin by Spatial Populations of Cutaneous Mechano-Nociceptors. Journal of Neurophysiology, 2000, 83, 3049-3061.	0.9	20
118	Nonlinear dependence of loading intensity and cycle number in the maintenance of bone mass and morphology. Journal of Orthopaedic Research, 1998, 16, 482-489.	1.2	198
119	Skeletal Cell Stresses and Bone Adaptation. American Journal of the Medical Sciences, 1998, 316, 176-183.	0.4	36
120	Whole-body vibration in the skeleton: Development of a resonance-based testing device. Annals of Biomedical Engineering, 1997, 25, 831-839.	1.3	55
121	Correlation of bony ingrowth to the distribution of stress and strain parameters surrounding a porous-coated implant. Journal of Orthopaedic Research, 1996, 14, 862-870.	1.2	39
122	Differentiation of the Bone-Tissue Remodeling Response to Axial and Torsional Loading in the Turkey Ulna*â€. Journal of Bone and Joint Surgery - Series A, 1996, 78, 1523-33.	1.4	111